Ind. J. Pharm. Edu. Res., 2025; 59(1):185-195.
https://www.ijper.org

Original Article

Propofol Inhibits Oxidative Stress-Induced Neuronal Cell Ferroptosis and Promotes Synaptic Plasticity via the AMPK/SIRT1/PGC-1α Axis

Rongmin Chen[1,#], Miao Zhang[2,#], Liangce Lv[2], Ruqiu Yin[3,*]

[1]Department of Anesthesiology, Huashan Hospital, Fudan University, Shanghai, CHINA.
[2]Department of Anesthesiology, Shanghai General Hospital Jiading Branch, Shanghai, CHINA.
[3]Department of Anesthesiology, Shanghai Eighth People's Hospital, Shanghai, CHINA.
[#]*Rongmin Chen and Miao Zhang contributed equally to this work.*

ABSTRACT

Aim/Background: Propofol, recognized for its quick and effective action as a hypnotic anesthetic, is frequently utilized in clinical practice. Our research intended to investigate the mechanism by which propofol inhibits neuronal ferroptosis and promotes synaptic plasticity via mitochondrial energy regulation. **Materials and Methods:** Mouse Hippocampal Neurons (HT22) cells were treated with RAS-Selective Lethal 3 (RSL3) and propofol followed by Reactive Oxygen species (ROS) detection. Expression levels of ferroptosis and mitochondrial energy regulation were analyzed. HT22 cells were treated with a Sirtuin 1 (SIRT1) inhibitor before propofol treatment. Level of ROS, Fe^{2+} and genes expression and synaptic plasticity were measured. **Results:** In the RSL3-Low+propofol cohort, exhibiting a stark contrast to both the mock group and the RSL3-High+propofol group, the administration of propofol notably attenuated the expression of ROS, Cyclooxygenase 2 (COX-2) and Long-chain-fatty-acid-CoA Ligase 4 (ACSL4), while concurrently enhancing the levels of Glutathione Peroxidase 4 (GPX4), Solute Carrier Family 7 Member 11 (SLC7A11), Nuclear Factor-like 2 (NRF2), Ferritin Heavy chain 1 (FTH1), Adenosine 5'-Monophosphate (AMP)-Activated Protein Kinase (AMPK), SIRT1 and PPARγ Coactivator-1α (PGC-1α). ROS and Fe^{2+} levels were substantially greater in the Selisistat+propofol group than in the propofol group, whereas SIRT1 and PGC-1α expression levels were considerably less in comparison to the mock and propofol groups. Conversely, the propofol group showed significantly higher levels of AMPK, SIRT1, PGC-1α, Synapsin-1 (SYN1) and PSD-95 compared to the mock group and the Selisistat+propofol group ($p<0.05$). **Conclusion:** Propofol inhibits oxidative stress-induced neuronal cell ferroptosis and promotes synaptic plasticity via the AMPK/SIRT1/PGC-1α axis.

Keywords: Ferroptosis, Oxidative stress, Propofol, Synaptic plasticity.

Correspondence:
Dr. Ruqiu Yin
Department of Anesthesiology,
Shanghai Eighth People's Hospital,
Shanghai, 200000, CHINA.
Email: yruqiu@126.com

Received: 25-09-2024;
Revised: 24-10-2024;
Accepted: 13-11-2024.

INTRODUCTION

Propofol, a commonly used sedative in clinical settings, offers rapid onset and control with minimal side effects.[1] It is recognized for its neuroprotective properties,[2,3] protecting the brain from ischemic damage through antioxidant activity, reducing free radicals and mitigating lipid peroxidation.[4] Studies reported that propofol regulates certain receptors to decrease neuronal damage in animal models of cerebral ischemia and to improve ferroptosis by down-regulating Hypoxia-Inducible Factor-1α (HIF-1α) in ischemia/reperfusion model of neurons.[5-7] Ferroptosis, a form of cell death characterized by Reactive Oxygen Species (ROS) accumulation and lipid peroxidation, can be influenced by propofol due to its chemical structure, which is similar to the antioxidant Vitamin E.[8,9] This allows it to react with ROS and reduce lipid peroxide production, thus playing a role in mitochondrial quality control and energy metabolism regulation. However, the underlying mechanisms behind propofol in improving neuron mitochondrial function or ferroptosis is not fully investigated yet. Therefore, further elucidating the mechanism of propofol is needed.

Peroxisome proliferator-activated receptor-gamma coactivator-1α (PGC-1α) is a major regulator of mitochondrial quality control, promoting mitochondrial biosynthesis and being regulated by SIRT1, an enzyme involved in nerve growth and oxidative stress response.[10] When mitochondrial damage results in an insufficient supply of energy for normal cellular activity,

DOI: 10.5530/ijper.20250931

Sirtuin 1 (SIRT1) enzyme activity increases, which promotes deacetylation of PGC-1α, leading to an increase in mitochondrial synthesis, which stabilizes the cellular state.[11] Adenosine 5'-Monophosphate (AMP)-Activated Protein Kinase (AMPK) directly phosphorylates the ser538 and Thr177 gene sites of PGC-1α, promotes the PGC-1α transcription.[12,13] The AMPK/SIRT1/PGC-1α signaling pathway is crucial for mitochondrial stability, integrating mitochondrial function sensing and energy output.[11,14] Studies have proved that propofol activates AMPK/mammalian target of Rapamycin (mTOR) pathway and SIRT3 enhances the protective effect of propofol by triggering autophagy to ameliorate postoperative cognitive dysfunction, indicating the potential property of propofol in modulating AMPK-related signaling.[15]

In this research, we investigate propofol's protective effects against oxidative stress in Hippocampal Neurons (HT22) cells, focusing on its ability to inhibit ferroptosis and promote synaptic plasticity through the AMPK/SIRT1/PGC-1α axis, by examining the expression levels of ferroptosis-related indicators and genes related to mitochondrial energy regulation and synaptic plasticity.

MATERIALS AND METHODS

Cell Cultivation and Chemicals

The murine hippocampal neuronal Mouse HT22 cell line was obtained from the American Type Culture Collection (ATCC) (Manassas, BFN60808571, VA, USA). The HT22 cells were cultivated in Dulbecco's Modified Eagle Medium (DMEM) sourced from Gibco (Rockville, A5669701, MD, USA), enriched with 10% Fetal Bovine Serum (FBS) also from Gibco and 100 units/mL penicillin/streptomycin from Sigma (St. Louis, V900929, MO, USA). The cells were maintained in a humidified, 5% CO_2 incubator at a temperature of at 37°C. We bought RAS-selective lethal 3 (RSL3) (MedChemExpress, HY-100218A, Monmouth Junction, NJ, USA), Propofol injection (MedChemExpress, HY-B0649, Monmouth Junction, NJ, USA) and Selisistat (MedChemExpress, HY-15452, Monmouth Junction, NJ, USA) from MedChemExpress (Monmouth Junction, NJ, USA). Glyceraldehyde-3-Phosphate Dehydrogenase (GAPDH) antibody (Abcam, [6C5] (ab8245), Cambridge, MA, USA), Glutathione Peroxidase 4 (GPX4) antibody (Abcam, [EPNCIR144] (ab125066), Cambridge, MA, USA), cysteine/glutamate antiporter (xCT) antibody (Abcam, [EPR8290(2)] (ab175186), Cambridge, MA, USA), Cyclooxygenase 2 (COX2) antibody (Abcam, [EPR12012] (ab179800), Cambridge, MA, USA), Long-chain-fatty-acid-CoA Ligase 4 (ACSL4) antibody (Abcam, [EPR8640] (ab155282), Cambridge, MA, USA), Nuclear factor-like 2 (NRF2) antibody (CST, #12721, Danvers, MA, USA), Ferritin heavy chain 1 (FTH1) antibody (CST, #3998, Danvers, MA, USA), Adenosine 5'-Monophosphate (AMP)-Activated Protein Kinase (AMPKα) antibody (CST, #2532, Danvers, MA, USA), Sirtuin 1 (SIRT1) antibody (CST, #9475, Danvers, MA, USA), PPARγ Coactivator-1α (PGC1α) antibody (CST, #4259, Danvers, MA, USA), postsynaptic density protein 95 (PSD95) antibody (Abcam, ab18258, Cambridge, MA, USA) and Synapsin-1 antibody (CST, #5297, Danvers, MA, USA) were purchased from Abcam (Cambridge, MA, USA). All utilized cells in this study were free from mycoplasma contamination.

Drug treatment

The Blank group did not use any treatments and the RSL3-Low and RSL3-High groups used 2 μmol/L or 10 μmol/L RSL3 (GPX4 inhibitor) to treat the HT22 cells for 8 hr, followed by a 6-hr exposure to 50 μmol/L propofol. The concentrations of 2 μmol/L and 10 μmol/L for RSL3 were selected based on preliminary experiments showing that these levels effectively induced varying degrees of ferroptosis without causing complete cell death. This range allowed for the observation of propofol's protective effects at different oxidative stress intensities. An 8-hr treatment duration with RSL3 was chosen to allow sufficient induction of ferroptosis-related markers, while a subsequent 6-hr exposure to propofol was found optimal for observing its neuroprotective effects (Figure 1A).[16,17]

In a separate experimental series, the mock group was treated with 5 μmol/L RSL3. The propofol group underwent an 8-hr treatment with 5 μmol/L RSL3 and a 6-hr exposure to 50 μmol/L propofol. The Selisistat (SIRT1 inhibitor)+propofol group was treated with 5 μmol/L RSL3 for 8 hr, followed by a 30-min treatment with 10 μmol/L Selisistat and then a 6-hr exposure to 50 μmol/L propofol (Figure 1B).[18]

RT-qPCR

Total RNA was extracted using the Vazyme Cell/Tissue Total RNA Isolation Kit V2, following the protocol provided by the manufacturer. RNA concentration and purity were measured using a NanoDrop spectrophotometer (Thermo Fisher Scientific, Waltham, MA, USA). Subsequently, the HiScript III 1st Strand cDNA Synthesis Kit from Vazyme (Nanjing, China) was employed to convert total RNA into cDNA according to manufacturer's instructions. The reaction was carried out at 42°C for 15 min, followed by inactivation at 85°C for 5 min. RT-qPCR was carried out using Taq Pro Universal SYBR qPCR Master Mix, also provided by Vazyme (Nanjing, China) and utilizing the CFX96 Touch 1855195 from Bio-Rad (Hercules, CA, USA). Each reaction was conducted in a 20 μL volume containing 10 μL of 2x SYBR Green Master Mix, 1 μL of each primer (10 μM), 2 μL of cDNA template and 6 μL of nuclease-free water. The thermal cycling conditions were as follows: initial denaturation at 95°C for 3 min, followed by 40 cycles of 95°C for 10 sec, 60°C for 30 sec and a final melting curve analysis from 60°C to 95°C to verify the specificity of the amplified products. Analysis of each sample was conducted in triplicate, with Glyceraldehyde-3-Phosphate Dehydrogenase (GAPDH) serving as a reference gene. The relative quantitative findings were determined using the

$2^{-\Delta\Delta CT}$ method. Sangon Biotech (Shanghai, China) designed and synthesized the primers used in RT-qPCR, as listed in Table 1.

Western blot

Total protein extraction was performed using a 5-12% SDS-PAGE gel, followed by transfer to a Polyvinylidene Fluoride (PVDF) membrane (IPVH00010, Thermo Fisher Scientific). The membrane was blocked using a 5% skimmed milk solution at 25°C for duration of 1 hr. 1 mL of the primary antibody (A1978 (Sigma-Aldrich), Sigma-Aldrich) diluted at 1:2000 was added for incubation at 4°C overnight. Afterward, the membrane was incubated with the secondary antibody (1:5000, 31430 (Thermo Fisher Scientific), Thermo Fisher Scientific) for 1 hr under ambient conditions. The chemiluminescence reagents were mixed in equal volumes of liquid A and liquid B (NCM Biotech, Shanghai, China). Before being detected using the JP-K6000 chemiluminescence imager (Jiapeng, Shanghai, China), the membranes were incubated for 5 min. Protein expression was analyzed using Image J software (National Institutes of Health, NIH) for optical density values.

Table 1: Real-Time PCR Oligonucleotide Sequences.

Gene name	Sequence (5′→3′)
GPX4	Forward 5'-GTGTGGTTTACGAATCCTGG-3'
	Reverse 5'-CACATTTCTACATTTTATTCCCACAAGG-3'
SLC7A11	Forward 5'-TGCAAGCTCACAGCAATTCTG-3'
	Reverse 5'-AGATCGGGACTGCTAATGAG-3'
COX-2	Forward 5'-CTACCCATTCCAACTTGGTC-3'
	Reverse 5'-GGGAGGGCAATTATGATAAGG-3'
ACSL4	Forward 5'-CTTCCTCTTAAGGCCGGGA-3'
	Reverse 5'-TTATCCAGAGTATCTGCTCCAG-3'
NRF2	Forward 5'-AATGATACCTAGAGTAGTTTGGAAGG-3'
	Reverse 5'-AAAGCTCCAGCCTCTTGGTTTC-3'
FTH1	Forward 5'-CTACTGGAACTGCACAAACTG-3'
	Reverse 5'-CTTAGCTCTCATCACCGTGT-3'
AMPK	Forward 5'-ACAGTTGGATGCAGATGCTG-3'
	Reverse 5'-CAGAATTTTCCTTGTCACAGGTGG-3'
SIRT1	Forward 5'-TCGTTTTGCAAACTGACACCTG-3'
	Reverse 5'-CCAAGCAGGTTTGTTTCAGG-3'
PGC-1α	Forward 5'-AGACAGGCTTGTGCTCAGG-3'
	Reverse 5'-CGCTTTCACCAATGCTCTTC-3'
SYN1	Forward 5'-ATGAGTCTTGTAAGCATTAGCACC-3'
	Reverse 5'-CTGCTTACAGACAAGTTTGAAAGG-3'
PSD-95	Forward 5'-GCCCTTTCTCCTTTCTTCTC-3'
	Reverse 5'-TTAGAGGAAAAAAGCCCACAGC-3'
GAPDH	Forward 5'-TTAGGTTCATCAGGTAAACTCAGG-3'
	Reverse 5'-TTCTCGGCCTTGACTGTGC-3'

Measurement of intracellular ROS

The DCFH-DA was diluted in a serum-free culture medium at a dilution factor of 1:1000. Each well was filled with 3 mL of diluted DCFH-DA and the cells were subjected to a 20-min incubation period at a temperature of 37°C. Remove the DCFH-DA working solution and subsequently add HBSS to wash the plate two times. 500 µL of 4',6-diamidino-2-phenylindole (DAPI) was added to each well and pictures were taken with a fluorescence microscope (Zeiss, Oberkochen, Germany).

Colorimetric detection of Fe^{2+}

After the cells have been treated, gather them in a centrifuge tube and dispose of the supernatant after centrifugation. Add 0.9 mL of buffer for every 1 million cells and then ultrasonically break the cells using a power setting of 200W, with 3-sec pulses of ultrasonication, 10-sec intervals and repeat the process 30 times. Perform centrifugation of the sample at 10,000 g for 10 min at a temperature of 4°C, followed by collection of the supernatant. The standard, working solution and color development solution were prepared. The Optical Density (OD) value of the sample at 593 nm was measured (E-BC-F101, Elabscience Biotechnology Co., Ltd.).

Cellular immunofluorescence

The specific operation of immunofluorescence is as follows: (1) HT22 cells in the logarithmic growth phase were seeded at a density of $1*10^6$ cells per well in a 6-well culture plate. Following cell adhesion, the cells were subjected to serum starvation for 12 hr prior to treatment according to the experimental groups. (2) The 6-well culture plates were removed and the supernatant was aspirated. The cells were gently rinsed with Phosphate-Buffered Saline (PBS) three times, followed by the addition of 1 mL of 4% paraformaldehyde for fixation on a rocking platform at 50 rpm for 20 min. (3) After aspirating the supernatant, the plates were gently rinsed with PBS three times and 1 mL of 0.25% Triton-X100 was added for permeabilization on a rocking platform at 50 rpm for 20 min. (4) The cells were rinsed gently with PBS three times and 1 mL of goat serum was added for blocking for 30 min. (5) After removal of the blocking solution, 1 mL of the primary antibody diluted at 1:200 was added for incubation at 4°C overnight. (6) The primary antibody was decanted and the wells were washed three times with Tris Buffered Saline Tween (TBST) for 5 min each. Subsequently, 1 mL of the secondary antibody diluted at 1:200 was added for incubation at room temperature in the dark on a rocking platform at 50 rpm for 1 hr. (7) The secondary antibody was aspirated and the wells were washed three times with TBST

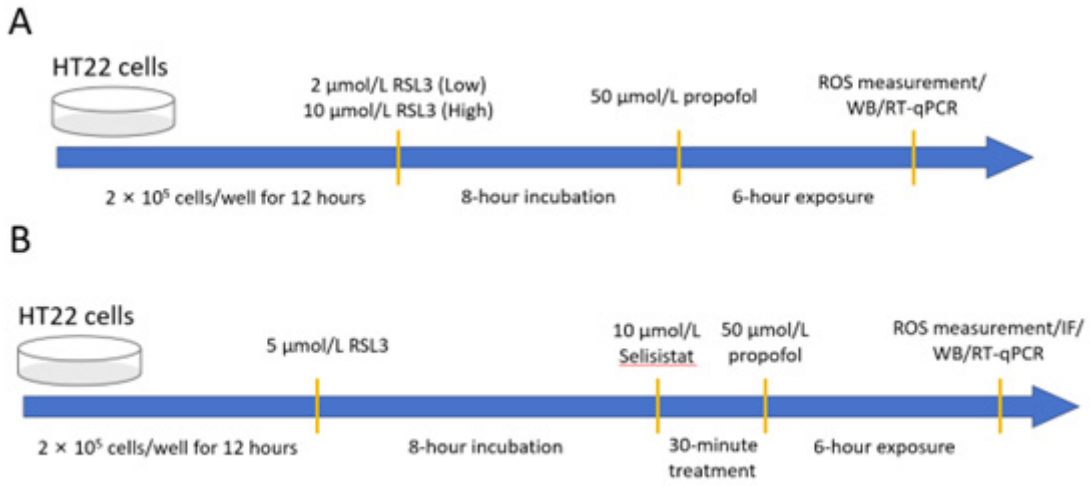

Figure 1: The workflow of experimental procedures.

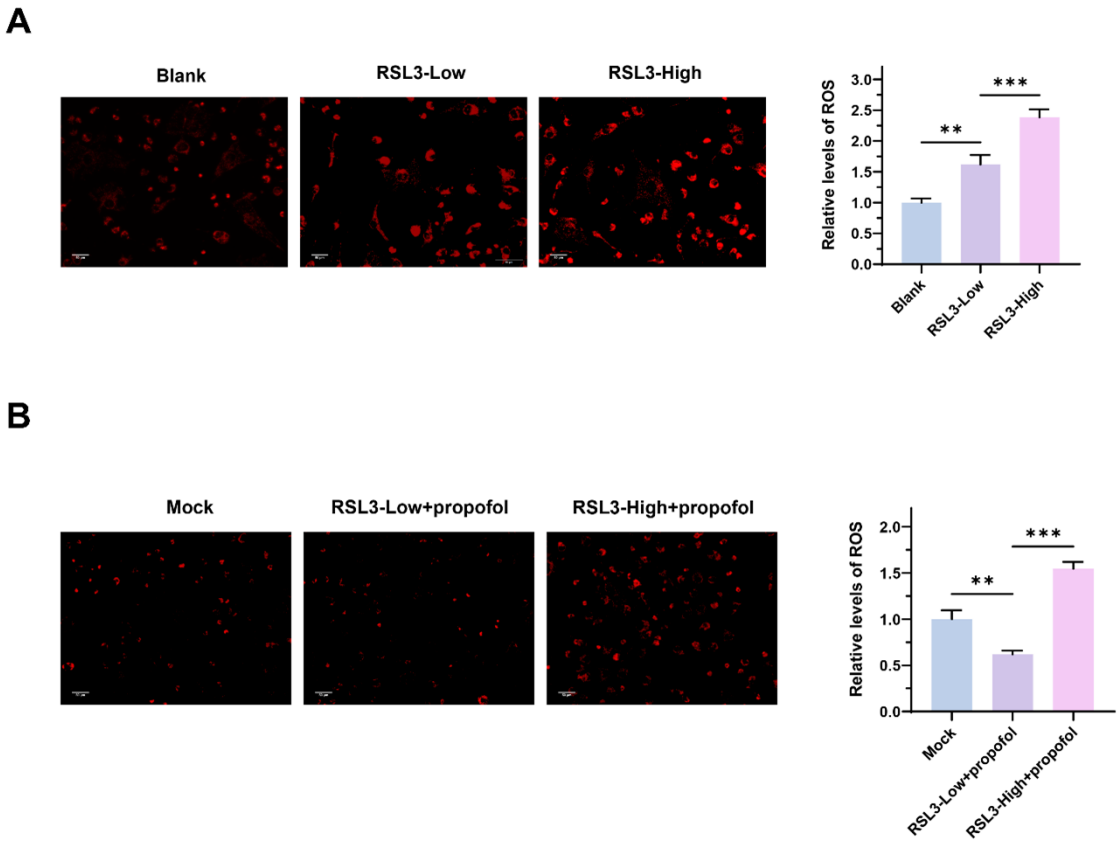

Figure 2: Effect of propofol on 2 μmol/L (low) and 10 μmol/L (High) RSL3-induced increase of ROS levels in HT22 cells. (A) ROS levels in HT22 cells resulting from different concentrations of RSL3. (B) Inhibitory effect of propofol on ROS levels resulting from different concentrations of RSL3. The blank group and the mock group were calibrated to 1. **p<0.01, ***p<0.001, n=3.

for 5 min each. The cells were then stained with DAPI for 5 min, after which the DAPI was aspirated and the wells were washed again with TBST three times for 5 min each. (8) The slides were mounted using Fluoroshield®®TM mounting medium containing DAPI and visualized under a fluorescence microscope. (9) Fluorescence intensity was quantified using Image J software.

Statistical analysis

Each experiment was performed independently on three occasions and the resultant data were expressed as mean±SD. ImageJ software was used to do grayscale analysis on Western Blot strips. GraphPad Prism 9 (La Jolla, CA, USA) was used to construct the representative graphs and Statistic Package for

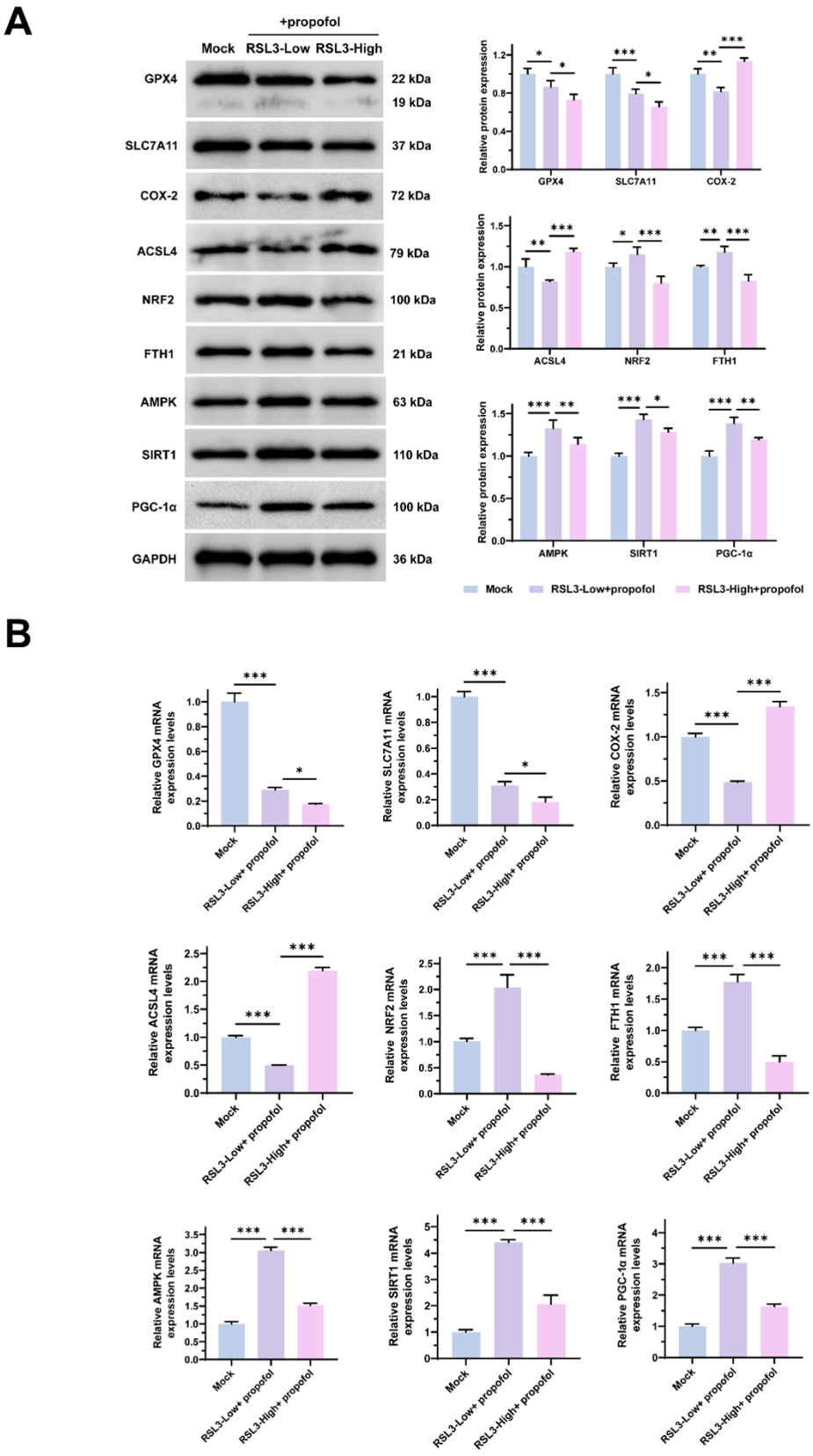

Figure 3: Effect of propofol on the expression levels of ferroptosis-related genes and AMPK/SIRT1/PGC-1α axis after 2 μmol/L (low) and 10 μmol/L (High) RSL3 treatment. (A) Protein levels of GPX4, SLC7A11, COX-2, ACSL4, NRF2, FTH1, AMPK, SIRT1 and PGC-1α. B. mRNA levels of GPX4, SLC7A11, COX-2, ACSL4, NRF2, FTH1, AMPK, SIRT1 and PGC-1α. The mock group were calibrated to 1. **p*<0.05, ***p*<0.01, ****p*<0.001, *n*=3.

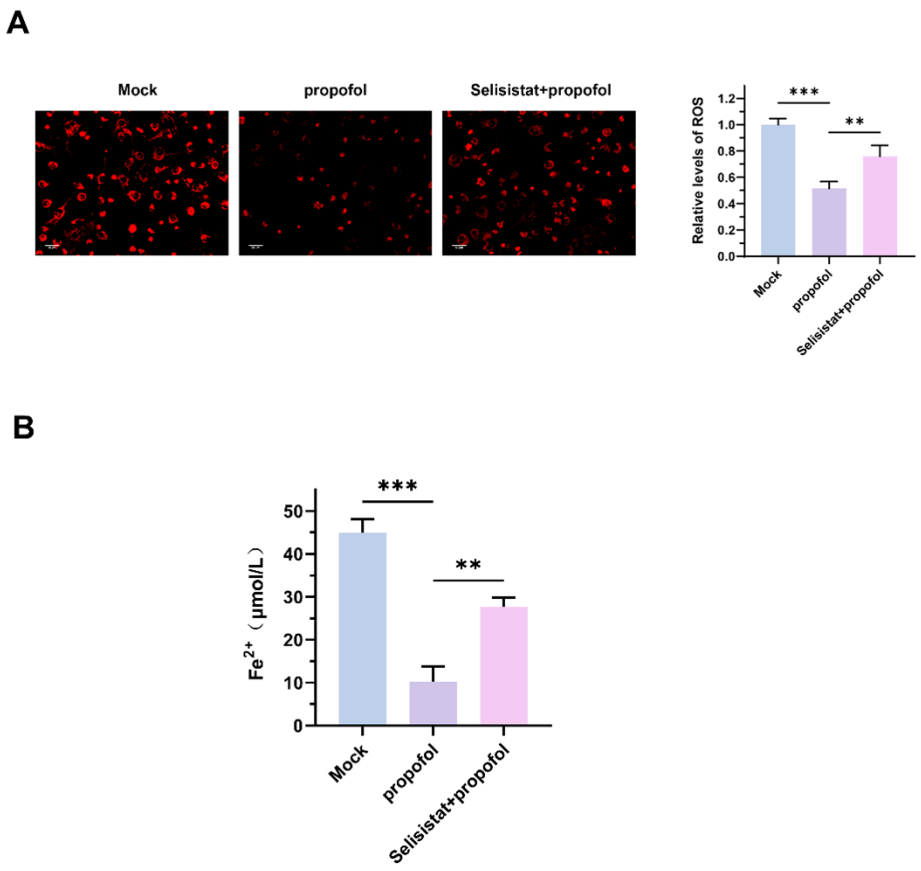

Figure 4: Effect of selisistat treatment on propofol downregulation of ROS and Fe^{2+} levels. (A) Effect of selisistat on ROS levels. (B) Effect of selisistat on Fe^{2+} concentration. The mock group were calibrated to 1. $^{**}p<0.01$, $^{***}p<0.001$, $n=3$.

Social Science (SPSS) 22.0 (IBM, Armonk, NY, USA) was used to analyze the data. A one-way ANOVA and *t*-tests were used to compare groups. To identify if there were significant differences, a $p<0.05$ statistical significance criterion was applied.

RESULTS

Propofol Attenuates RSL3-Induced ROS Elevation in HT22 Cells

Compared with Blank group, ROS levels were significantly increased in HT22 cells in RSL3-Low group and RSL3-High group, compared with RSL3-Low group, the ROS levels were significantly higher in RSL3-High group (Figure 2A). After adding 50 μmol/L propofol to RSL3-treated HT22 cells, propofol significantly lowered the ROS levels in the group treated with a low dose of RSL3 and had no significant effect on the RSL3-high group ($p<0.05$) (Figure 2B). Results suggested that propofol mitigated RSL3-induced ROS in HT22 cells at low doses but not at high doses.

Propofol inhibited RSL3-induced ferroptosis and promoted AMPK/SIRT1/PGC-1α axis activation

RSL3-Low+propofol group and the RSL3-High+propofol group showed lower GPX4 and SLC7A11 protein expression levels. Upon Propofol administration, the RSL3-Low+Propofol group experienced a notable upregulation in the protein levels of NRF2, FTH1, AMPK, SIRT1 and PGC-1α, as evidenced by western blot analysis, when contrasted with both the mock group and the RSL3-High+Propofol group. Furthermore, in the RSL3-Low+Propofol group, Propofol treatment resulted in a significant downregulation of COX-2 and ACSL4 protein expression in comparison to the mock group and the RSL3-High+Propofol group (Figure 3A) ($p<0.05$).

Compared with the mock group, RT-qPCR analysis revealed that RSL3 treatment significantly decreased the mRNA expression levels of GPX4 and SLC7A11. Compared to the mock group and the RSL3-High+propofol group, propofol administration substantially decreased the mRNA expression of COX-2 and ACSL4 in the RSL3-Low+propofol group. The RSL3-High+propofol group showed lower mRNA expression levels of NRF2 and FTH1 compared to the mock group and

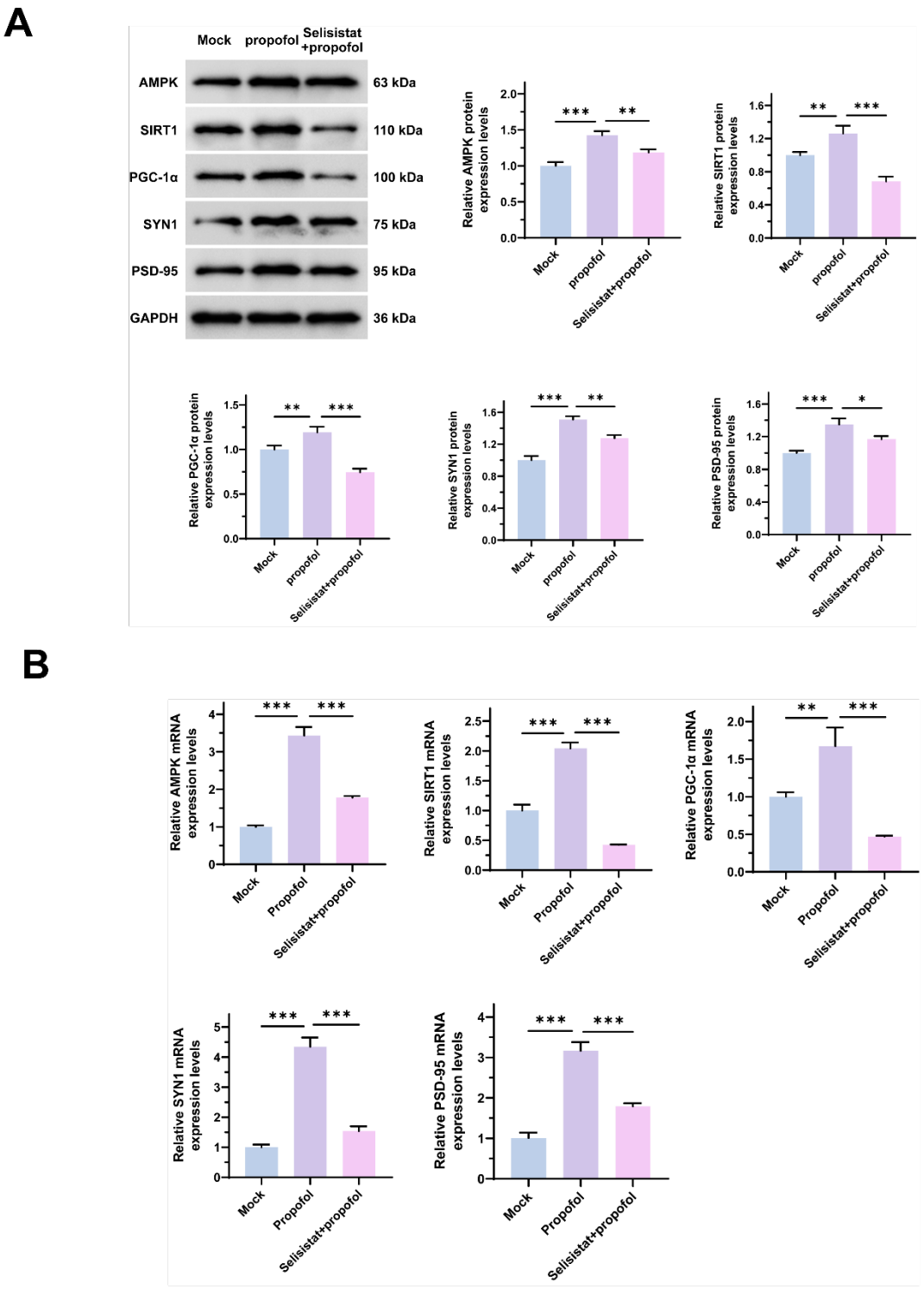

Figure 5: Propofol's Modulation of Synaptic Plasticity Proteins and mRNA through the AMPK/SIRT1/PGC-1α Axis. (A) Protein Expression Assessed by Western Blot for AMPK, SIRT1, PGC-1α, SYN1 and PSD-95. (B) mRNA Expression Assessed by RT-qPCR for AMPK, SIRT1, PGC-1α, SYN1 and PSD-95. The mock group were calibrated to 1. *p<0.05, **p<0.01, ***p<0.001, n=3.

the RSL3-Low+propofol group. The mRNA expression levels of NRF2, FTH1, AMPK, SIRT1 and PGC-1α were significantly elevated in the RSL3-Low+Propofol group relative to both the mock group and the RSL3-High+Propofol group (Figure 3B) (p<0.05). Results suggested that propofol induced gene and protein expression changes in RSL3-treated HT22 cells, with beneficial effects in the low-dose group and reduced efficacy in the high-dose group.

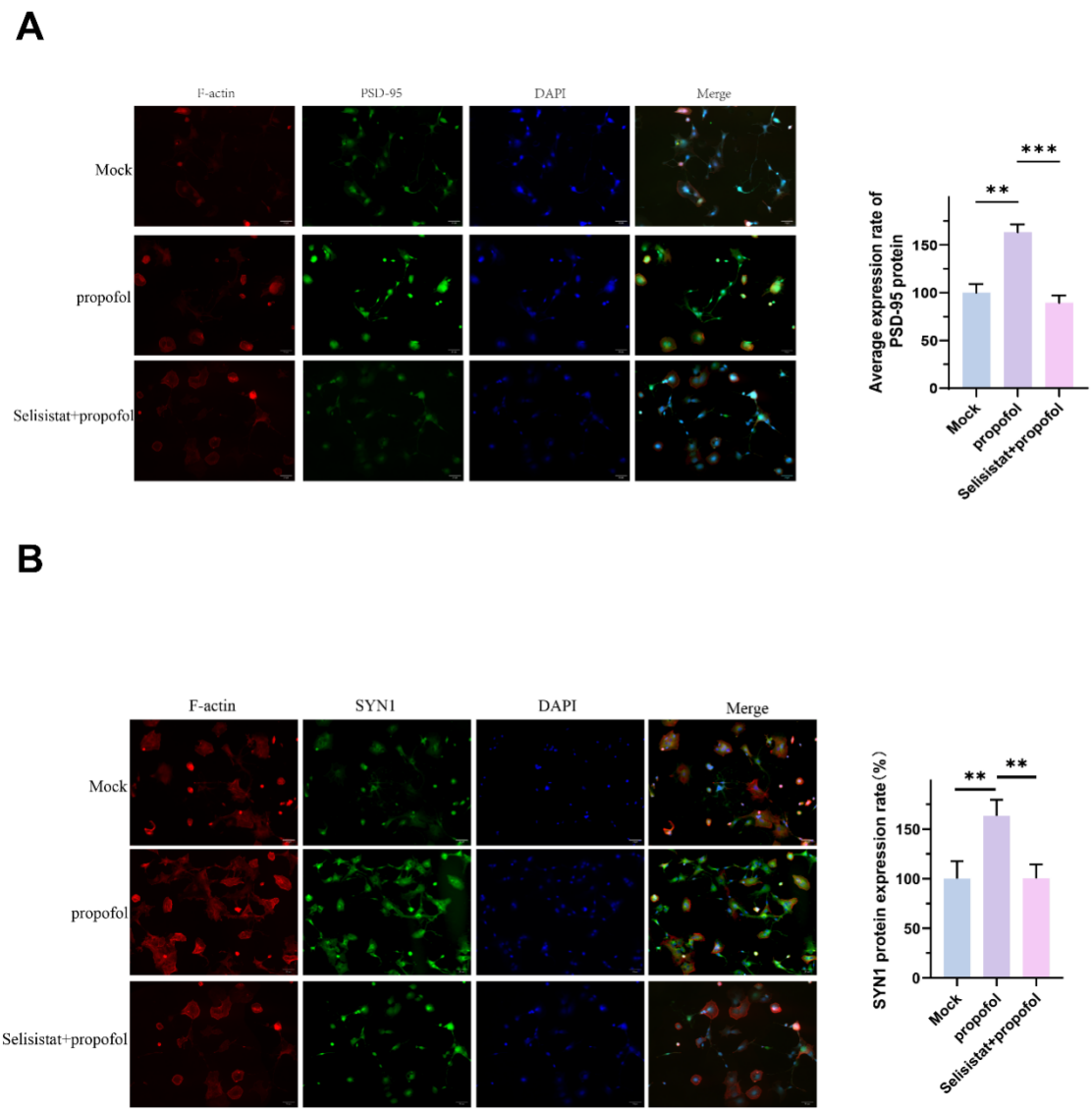

Figure 6: Propofol's Impact on the Localization and Expression of Synaptic Plasticity-Related Proteins. (A) PSD-95 Localization and Expression. (B) SYN1 Localization and Expression. The mock group were calibrated to 1. **p<0.01, ***p<0.001, n=3.

SIRT1 inhibitor suppressed the ability of propofol to inhibit ferroptosis

Propofol group showed Lower expression levels of ROS compared to the mock and the Selisistat+propofol group. Within the Selisistat+propofol group, when HT22 cells were first treated with selisistat, the inhibitory effect of propofol on ROS generation was diminished as compared to the propofol group (Figure 4A). Compared with the mock group and the Selisistat+propofol group, propofol group showed lower expression levels of Fe^{2+}. The Selisistat+propofol group exhibited greater Fe^{2+} levels in comparison to the group treated with propofol (Figure 4B) (p<0.05).

Propofol promoted the expression of synaptic plasticity-associated genes through AMPK/SIRT1/PGC-1α axis

The propofol group exhibited elevated protein levels for AMPK, SIRT1, PGC-1α, SYN1 and PSD-95, surpassing those observed in both the mock and Selisistat+propofol groups. Within the group of Selisistat+propofol, we first treated HT22 cells with selisistat and then added propofol for treatment. We discovered that the Selisistat+propofol group showed a significant reduction in protein expression levels of AMPK, SIRT1, PGC-1α, SYN1 and PSD-95 compared with the propofol group. In comparison to the mock and propofol groups, we found that the Selisistat+propofol group's protein expression levels of SIRT1 and PGC-1α significantly decreased as a result of treatment with the SIRT1 inhibitor (Figure 5A) (p<0.05).

RT-qPCR analysis demonstrated that, in comparison to the mock and Selisistat+propofol groups, treatment with propofol resulted in markedly increased mRNA expression across key synaptic plasticity proteins, including AMPK, SIRT1, PGC-1α, SYN1 and PSD-95. Selisistat mitigated the propofol's promotion of mRNA expression for AMPK, SIRT1, PGC-1α, SYN1 and PSD-95, with the Selisistat+propofol group exhibiting notably reduced mRNA levels of SIRT1 and PGC-1α relative to both the mock and propofol groups (Figure 5B) ($p<0.05$). Results suggested that Propofol increased the expression of synaptic plasticity proteins in HT22 cells, but this effect was reversed by prior treatment with the SIRT1 inhibitor selisistat.

Propofol promoted the expression of synaptic plasticity-associated proteins

Immunofluorescence was used to examine PSD-95 and SYN1 expression and localization in HT22 cells. The results showed that fluorescence signals for PSD-95 and SYN1 were notably enhanced in the propofol group, surpassing those in both the mock group and the Selisistat+propofol group. We first treated HT22 cells with selisistat and then added propofol treatment and the expression levels of PSD-95 and SYN1 within the Selisistat+propofol group exhibited no significant deviation from those observed in the mock group (Figure 6A-B) ($p<0.05$). Results suggested that propofol increased PSD-95 and SYN1 expression in HT22 cells, but this effect was abolished by prior selisistat treatment.

DISCUSSION

In this research, we investigate propofol's protective effects against oxidative stress in HT22 cells and its ability to inhibit ferroptosis and promote synaptic plasticity through the AMPK/SIRT1/PGC-1α axis, by examining the expression levels of ferroptosis-related indicators and genes related to mitochondrial energy regulation and synaptic plasticity.

Propofol, a frequently utilized intravenous anesthetic, finds extensive application across diverse clinical environments.[19] Propofol's primary site of action is the synapse and its primary mechanism of propofol anesthesia is to block the release of presynaptic membrane transmitters.[20] Propofol's neuroprotective functions have been shown to significantly rescue neuronal damage in neuronal inflammation caused by cerebral ischemia and brain injury.[21] Our study suggests that propofol can mitigate oxidative stress and inhibit ferroptosis in neuronal cells via the AMPK/SIRT1/PGC-1α axis, mechanisms that are relevant for neuroprotection. These findings imply that propofol may have potential clinical applications beyond anesthesia, including the prevention of neuronal damage in conditions such as ischemic brain injury and neurodegenerative diseases like Alzheimer's and Parkinson's. Given the association between ferroptosis and neurodegenerative disorders, the inhibition of ferroptosis by propofol could offer a novel therapeutic strategy. However, translation to clinical practice will require further *in vivo* studies to confirm the efficacy of propofol in animal models of neurodegeneration, followed by clinical trials to determine optimal dosages and long-term effects.

Recent years have shown a strong association between ferroptosis and neurodegenerative diseases.[22] Ferroptosis leads to a significant buildup of iron-dependent,-lethal lipid ROS, potentially triggering an inflammatory response within the central nervous system.[23] Evidence suggests that propofol, when used clinically, effectively reduces the excessive lipid oxidation induced by H_2O_2 and its lower concentrations have been demonstrated to exert a protective effect on cell membrane.[24] Good lipid-soluble propofol can be assembled at the cell membrane to enhance the resistance to ROS. Propofol also suppresses superoxide radicals produced by H_2O_2 from inactivating NF-κB, which may protect cells in an indirect manner.[25] In the current investigation, we observed that propofol possesses anti-ROS capabilities and can suppress ferroptosis.

Research has demonstrated that frequent exposure to propofol can negatively affect synaptic plasticity and recognition function.[26,27] Studies also have indicated that propofol can augment cognitive functions, specifically improving memory retention and cognitive learning capabilities in rats exhibiting symptoms of Post-Traumatic Stress Disorder (PTSD), through the restoration of synaptic plasticity in the hippocampus.[28] But most studies have focused on the area of propofol against neuronal damage, such as neurodegenerative diseases and brain dysfunction.[29,30] In the present study, we determined that propofol promotes synaptic plasticity, possibly through the regulation of neuronal intracellular energy via the AMPK/SIRT1/PGC-1α axis. Activation of the AMPK/SIRT1/PGC-1α pathway is integral to reducing oxidative stress, inhibiting apoptosis and averting mitochondrial fission.[31,32]

To explore the inhibitory impact of propofol on ferroptosis in neuronal cells, we treated HT22 cells with RSL3, a ferroptosis inducer, at varying concentrations and observed that higher concentrations led to increased ROS generation. We observed that when a specific concentration of propofol was given to HT22 cells that had been treated with varying concentrations of RSL3, the generation of ROS was inhibited. It is possible that propofol was not sufficient to inhibit oxidative stress in the high-concentration RSL3 group due to the concentration and treatment time. Propofol suppressed the expression of genes associated with ferroptosis onset and the AMPK/SIRT1/PGC signaling pathway's activity was activated. Propofol facilitated the expression of genes associated with synaptic plasticity and that synaptic plasticity involved the AMPK/SIRT1/PGC-1α axis.

The AMPK/SIRT1/PGC-1α axis is a promising target for neuroprotection, with implications for treating neurodegenerative diseases. AMPK activation can protect neurons by regulating

metabolism and reducing oxidative stress. SIRT1 and PGC-1α enhance mitochondrial function and biogenesis, crucial for neuronal health.[33,34] It has been proven that propofol inhibits ferroptosis in the hippocampus of postoperative cognitive dysfunction rats by improving the downregulation of SIRT1/Nrf2/GPX4 pathway, indicating the effects of propofol in regulating SIRT1-related signaling pathway mediated ferroptosis.[35] In accordance with previous reports, we found that propofol is able to ameliorate neuronal ferroptosis by modulating AMPK/SIRT1/PGC-1α axis in the present research. Propofol's modulation of this axis inhibits ferroptosis and promotes synaptic plasticity, suggesting its potential in enhancing cognitive function and combating neurodegeneration. While the study provides valuable insights, clinical translation requires further research to determine optimal dosage and potential side effects. A combination therapy approach targeting this axis, alongside other pathways, may offer effective treatment strategies.

Our findings highlight the potential of propofol not only as an anesthetic but also as a neuroprotective agent. However, this study had some limitations. In subsequent experiments, we will validate our results using animal models of neurological damage and investigate the AMPK/SIRT1/PGC-1α axis's role in the neuroprotective properties of propofol. In addition, the potential biases in the experimental design and limitations of the detection methods existed in our manuscript. Future research directions should be suggested to address these limitations and validate the findings in larger, independent cohorts. Also, future research should focus on validating these *in vitro* findings in animal models and exploring the AMPK/SIRT1/PGC-1α axis as a therapeutic target for neuroprotection. Ultimately, the integration of propofol or its derivatives into clinical practice for managing neurodegenerative conditions could represent a significant advancement in the field of neuroprotection.

CONCLUSION

In summary, we have shown that propofol has a function in neuronal cell ferroptosis. Propofol may inhibit oxidative stress-induced neuronal cell ferroptosis and promote synaptic plasticity via the AMPK/SIRT1/PGC-1α axis. It may reduce oxidative neuronal death and enhance cognitive functions by modulating mitochondrial energy regulation and synaptic markers. This highlights propofol's potential in treating cognitive decline in neurodegenerative diseases.

AUTHOR CONTRIBUTIONS

Rongmin Chen, Ruqiu Yin: Conceptualization, methodology, writing original draft preparation. Liangce Lv: Investigation, software, statistical analysis. Miao Zhang: Reviewing and editing, funding acquisition, supervision. All authors read and approved the final manuscript.

CONFLICT OF INTEREST

The authors declare that there is no conflict of interest.

ABBREVIATIONS

GPX4: Glutathione Peroxidase 4; **SLC7A11:** Solute Carrier Family 7 Member 11; **COX-2:** Cyclooxygenase 2; **ACSL4:** Long-chain-fatty-acid-CoA ligase 4; **NRF2:** Nuclear factor-like 2; **FTH1:** Ferritin heavy chain 1; **AMPK:** Adenosine 5‘-monophosphate (AMP)-activated protein kinase; **SIRT1:** Sirtuin 1; **PGC-1α:** PPARγ coactivator-1α; **SYN1:** Synapsin-1; **PSD-95:** Postsynaptic density protein 95; **GAPDH:** Glyceraldehyde-3-phosphate dehydrogenase; species were from mus musculus.

REFERENCES

1. Zheng H, Xiao X, Han Y, Wang P, Zang L, Wang L, *et al.* Research progress of propofol in alleviating cerebral ischemia/reperfusion injury. Pharmacol Rep. 2024;76(5):962-80. doi: 10.1007/s43440-024-00620-6, PMID 38954373.
2. Yu S, Xin W, Jiang Q, Li A. Propofol exerts neuroprotective functions by down-regulating microRNA-19a in glutamic acid-induced PC12 cells. BioFactors. 2020;46(6):934-42. doi: 10.1002/biof.1607, PMID 31913544.
3. Burnett GW, Taree A, Martin L, Bryson EO. Propofol misuse in medical professions: a scoping review. Can J Anaesth. 2023;70(3):395-405. doi: 10.1007/s12630-022-02382-2, PMID 36577890.
4. Tang Y, Gao X, Xu J, Ren L, Qi H, Li R, *et al.* Remimazolam besylate versus propofol for deep sedation in critically ill patients: a randomized pilot study. Crit Care. 2023;27(1):474. doi: 10.1186/s13054-023-04760-8, PMID 38049909.
5. Ma Z, Li K, Chen P, Pan J, Li X, Zhao G. Propofol attenuates inflammatory damage via inhibiting NLRP1-Casp1-Casp6 signaling in ischemic brain injury. Biol Pharm Bull. 2020;43(10):1481-9. doi: 10.1248/bpb.b20-00050, PMID 32999158.
6. Wang Y, Tian D, Wei C, Cui V, Wang H, Zhu Y, *et al.* Propofol attenuates alpha-synuclein aggregation and neuronal damage in a mouse model of ischemic stroke. Neurosci Bull. 2020;36(3):289-98. doi: 10.1007/s12264-019-00426-0, PMID 31520398.
7. Ma H, Ye D, Liu Y, Wu P, Yu L, Guo L, *et al.* Propofol suppresses OGD/R-induced ferroptosis in neurons by inhibiting the HIF-1alpha/YTHDF1/BECN1 axis. Brain Inj. 2023;37(11):1285-93. doi: 10.1080/02699052.2023.2237881, PMID 37614036.
8. Van S, Lam V, Patel K, Humphries A, Siddiqi J. Propofol-related infusion syndrome: A bibliometric analysis of the 100 most-cited articles. Cureus. 2023;15(10):e46497. doi: 10.7759/cureus.46497, PMID 37927719.
9. Li J, Yu W, Li XT, Qi SH, Li B. The effects of propofol on mitochondrial dysfunction following focal cerebral ischemia-reperfusion in rats. Neuropharmacology. 2014;77:358-68. doi: 10.1016/j.neuropharm.2013.08.029, PMID 24035920.
10. Guan S, Sun L, Wang X, Huang X, Luo T. Propofol inhibits neuroinflammation and metabolic reprogramming in microglia *in vitro* and *in vivo*. Front Pharmacol. 2023;14:1161810. doi: 10.3389/fphar.2023.1161810, PMID 37383725.
11. Yang X, Liu Q, Li Y, Tang Q, Wu T, Chen L, *et al.* The diabetes medication canagliflozin promotes mitochondrial remodelling of adipocyte via the AMPK-Sirt1-Pgc-1alpha signalling pathway. Adipocyte. 2020;9(1):484-94. doi: 10.1080/21623945.2020.1807850, PMID 32835596.
12. Hu M, Jiang W, Ye C, Hu T, Yu Q, Meng M, *et al.* Honokiol attenuates high glucose-induced peripheral neuropathy via inhibiting ferroptosis and activating AMPK/SIRT1/PGC-1alpha pathway in Schwann cells. Phytother Res. 2023;37(12):5787-802. doi: 10.1002/ptr.7984, PMID 37580045.
13. Cantó C, Auwerx J. PGC-1alpha, SIRT1 and AMPK, an energy sensing network that controls energy expenditure. Curr Opin Lipidol. 2009;20(2):98-105. doi: 10.1097/MOL.0b013e328328d0a4, PMID 19276888.
14. Meng H, Wang QY, Li N, He H, Lu WJ, Wang QX, *et al*. Danqi Tablet Regulates Energy Metabolism in Ischemic Heart Rat Model through AMPK/SIRT1-PGC-1alpha Pathway. Chin J Integr Med. 2021;27(8):597-603. Available from: https://pubmed.ncbi.nlm.nih.gov/31144160/.
15. Li S, Zhou Y, Hu H, Wang X, Xu J, Bai C, *et al.* SIRT3 enhances the protective role of propofol in postoperative cognitive dysfunction via activating autophagy mediated by AMPK/mTOR pathway. Front Biosci (Landmark Ed). 2022;27(11):303. doi: 10.31083/j.fbl2711303, PMID 36472103.
16. Zhang B, Hou Q, Zhang X, Ma Y, Yuan J, Li S, *et al.* Anesthetic propofol inhibits ferroptosis and aggravates distant cancer metastasis via Nrf2 upregulation. Free Radic Biol Med. 2023;195:298-308. doi: 10.1016/j.freeradbiomed.2022.12.092, PMID 36586453.
17. Fan GB, Li Y, Xu GS, Zhao AY, Jin HJ, Sun SQ, *et al.* Propofol inhibits ferroptotic cell death through the Nrf2/Gpx4 signaling pathway in the mouse model of cerebral

ischemia-reperfusion injury. Neurochem Res. 2023;48(3):956-66. doi: 10.1007/s11064-022-03822-7, PMID 36402927.

18. Zhang XS, Lu Y, Li W, Tao T, Wang WH, Gao S, *et al.* Cerebroprotection by dioscin after experimental subarachnoid haemorrhage via inhibiting NLRP3 inflammasome through SIRT1-dependent pathway. Br J Pharmacol. 2021;178(18):3648-66. doi: 10.1111/bph.15507, PMID 33904167.
19. Zhu XN, Li J, Qiu GL, Wang L, Lu C, Guo YG, *et al.* Propofol exerts anti-anhedonia effects via inhibiting the dopamine transporter. Neuron. 2023;111(10):1626-1636.e6. doi: 10.1016/j.neuron.2023.02.017, PMID 36917979.
20. Guidi M, Csajka C, Buclin T. Parametric approaches in population pharmacokinetics. J Clin Pharmacol. 2022;62(2):125-41. doi: 10.1002/jcph.1633, PMID 33103774.
21. Hu F, Jiang J, Yu G, Zang H, Sun H. Propofol pretreatment prevents oxygen-glucose deprivation/reoxygenation (OGD/R)-induced inflammation through nuclear transcription factor kappaB (NF-kappaB) pathway in neuroblastoma cells. Curr Neurovasc Res. 2020;17(1):27-34. doi: 10.2174/1567202617666191227110158, PMID 31880261.
22. Reichert CO, de Freitas FA, Sampaio-Silva J, Rokita-Rosa L, Barros PL, Levy D, *et al.* Ferroptosis mechanisms involved in neurodegenerative diseases. Int J Mol Sci. 2020;21(22):8765. doi: 10.3390/ijms21228765, PMID 33233496.
23. Zeng F, Nijiati S, Tang L, Ye J, Zhou Z, Chen X. Ferroptosis detection: from approaches to applications. Angew Chem Int Ed Engl. 2023;62(35):e202300379. doi: 10.1002/anie.202300379, PMID 36828775.
24. Kotani Y, Pruna A, Turi S, Borghi G, Lee TC, Zangrillo A, *et al.* Propofol and survival: an updated meta-analysis of randomized clinical trials. Crit Care. 2023;27(1):139. doi: 10.1186/s13054-023-04431-8, PMID 37046269.
25. Li S, Lei Z, Zhao M, Hou Y, Wang D, Xu X, *et al.* Propofol inhibits ischemia/reperfusion-induced cardiotoxicity through the protein kinase C/nuclear factor erythroid 2-related factor pathway. Front Pharmacol. 2021;12:655726. doi: 10.3389/fphar.2021.655726, PMID 34054535.
26. Wan J, Shen CM, Wang Y, Wu QZ, Wang YL, Liu Q, *et al.* Repeated exposure to propofol in the neonatal period impairs hippocampal synaptic plasticity and the recognition function of rats in adulthood. Brain Res Bull. 2021;169:63-72. doi: 10.1016/j.brainresbull.2021.01.007, PMID 33450329.
27. Duan J, Ju X, Wang X, Liu N, Xu S, Wang S. Effects of remimazolam and propofol on emergence agitation in elderly patients undergoing hip replacement: A clinical, randomized, controlled study. Drug Des Dev Ther. 2023;17:2669-78. doi: 10.2147/DDDT.S419146, PMID 37680862.
28. Niu W, Duan Y, Kang Y, Cao X, Xue Q. Propofol improves learning and memory in post-traumatic stress disorder (PTSD) mice via recovering hippocampus synaptic plasticity. Life Sci. 2022;293:120349. doi: 10.1016/j.lfs.2022.120349, PMID 35065162.
29. Ji D, Karlik J. Neurotoxic impact of individual anesthetic agents on the developing brain. Children (Basel). 2022;9(11):1779. doi: 10.3390/children9111779, PMID 36421228.
30. Bhattacharya S, Donoghue JA, Mahnke M, Brincat SL, Brown EN, Miller EK. Propofol anesthesia alters cortical traveling waves. J Cogn Neurosci. 2022;34(7):1274-86. doi: 10.1162/jocn_a_01856, PMID 35468201.
31. Gao J, Qian T, Wang W. CTRP3 activates the AMPK/SIRT1-PGC-1alpha pathway to protect mitochondrial biogenesis and functions in cerebral ischemic stroke. Neurochem Res. 2020;45(12):3045-58. doi: 10.1007/s11064-020-03152-6, PMID 33098065.
32. Li Q, Wu J, Huang J, Hu R, You H, Liu L, *et al.* Paeoniflorin ameliorates skeletal muscle atrophy in chronic kidney disease via AMPK/SIRT1/PGC-1alpha-Mediated oxidative stress and mitochondrial dysfunction. Front Pharmacol. 2022;13:859723. doi: 10.3389/fphar.2022.859723, PMID 35370668.
33. Jin T, Zhang Y, Botchway BO, Huang M, Lu Q, Liu X. Quercetin activates the Sestrin2/AMPK/SIRT1 axis to improve amyotrophic lateral sclerosis. Biomed Pharmacother. 2023;161:114515. doi: 10.1016/j.biopha.2023.114515, PMID 36913894.
34. Rakshe PS, Dutta BJ, Chib S, Maurya N, Singh S. Unveiling the interplay of AMPK/SIRT1/PGC-1alpha axis in brain health: promising targets against aging and NDDs. Ageing Res Rev. 2024;96:102255. doi: 10.1016/j.arr.2024.102255, PMID 38490497.
35. Wen Y, Zhang W, Wang D, Lu M. Propofol ameliorates cognitive deficits following splenectomy in aged rats by inhibiting ferroptosis via the SIRT1/Nrf2/GPX4 pathway. NeuroReport. 2024;35(13):846-56. doi: 10.1097/WNR.0000000000002074, PMID 38968575.

Cite this article: Chen R, Yin R, Zhang M, Liangce Lv. Propofol Inhibits Oxidative Stress-Induced Neuronal Cell Ferroptosis and Promotes Synaptic Plasticity via the AMPK/SIRT1/PGC-1α Axis. Indian J of Pharmaceutical Education and Research. 2025;59(1):185-95.